Pramana – J. Phys., Vol. 39, No. 2, August 1992, pp. 163–176. © Printed in India.

The inductively coupled plasma spectrum of OD in the infrared

MARK C ABRAMS[1,1a], SUMNER P DAVIS[1], M L P RAO[1,2] and ROLF ENGLEMAN JR[3]

[1]Department of Physics, University of California at Berkeley, Berkeley, California 94720, USA
[1a]Present address: ATMOS Data Analysis Facility, Jet Propulsion Laboratory, California Institute of Technology, 4800 Oak Grove Drive, Pasadena, CA 91109, USA
[2]Permanent address: Physics Department, Andhra University, Waltair 530003, India
[3]Department of Chemistry, University of Arizona – Tucson, Tucson, Az. 85721, USA

MS received 3 July 1990; revised 6 February 1992

Abstract. To gain more information about the highly excited rotational states of the $\Delta v = 1$ sequence of OD vibration-rotation bands, the spectrum has been produced in an inductively coupled plasma discharge and measured with a Fourier transform spectrometer between 1670 and 5768 cm^{-1}. Along with the extension of 1–0 band, we have been successful in recording the 2–1 band for the first time. A nonlinear least square fit of these bands yielded equilibrium molecular parameters for $v = 0, 1$ and 2 levels with a standard deviation of 0·0032 cm^{-1}. The centrifugal distortion parameters show a systematic vibrational dependance.

Keywords. OD rot-vib. spectrum; ICP discharge; centrifugal distortion constants.

PACS No. 33·20

1. Introduction

The spectrum of the OD free radical has been studied because of the presence of the hydroxyl radical in terrestrial, atmospheric and astronomical chemical systems. OH emission is characteristic of hydrocarbon flames and has been utilized to measure rotational temperatures in flames. The infrared nightglow in the upper atmosphere is dominated by OH vibration-rotation emission, and the formation of OH plays a central role in atmospheric chemistry.

In addition, the continuing refinement of *ab initio* calculations of the electronic structure of OD stimulates continuing spectroscopic interest. As the accuracy of calculations continues, improved spectroscopic data are critical for definitive testing of the theory. Many calculations of the fine structure and lambda-doubling splitting have been performed using both phenomenological and operator techniques for the $X^2\Pi$ ground state of OD. However, even for the ground state the experimental spectroscopic data are incomplete.

In the past decade several high resolution spectroscopic studies have provided detailed measurements of the transition frequencies of the spectra of the OH and OD radicals. Amiot *et al* (1981) observed 7 bands in the $\Delta v = 2$ sequence of OD emission in an deuterium oxygen flame. The Λ-doubling transitions in the ground state have been measured by Brown *et al* (1978) using electron paramagnetic resonance (EPR) techniques. The EPR work was refined with laser magnetic resonance of the OH

radical by Brown *et al* (1981) and extended to OD by Brown and Schubert (1982). Measurements were made on the fundamental vibration-rotation bands of OH and OD by Amano (1984) using difference frequency laser spectroscopy which resolved several satellite lines.

In the present paper, the infrared spectrum of OD has been extended to include an additional 96 lines from high J levels in the 1–0 band. We have been successful in recording the 2–1 band for the first time. We observed several P lines of the 3–2 band but no R lines. The spectral lines of the 1–0 and 2–1 bands were subjected to a simultaneous nonlinear least square fit to determine improved molecular parameters. The parameters determined with the nonlinear fit display a slow variation with vibrational quantum number, in particular the values of A_D for $v = 0, 1$, and 2 are all negative whereas in earlier works there was no pattern in the variation of the equilibrium parameters. This systematic vibrational dependance confirms the necessity of recording the spectra up to high J levels.

2. Experimental

The inductively coupled plasma is a high temperature source that combines the power of a microwave discharge with an atmospheric flowing argon gas torch. The central plasma reaches temperatures around 6000 K, sufficiently hot to dissociate the molecular reactants; typically molecular spectra are formed in the outer regions of the flame where temperature has decreased to a level where molecular formation can occur. The spectrum of OD was produced by bubbling the argon nebulizer gas flow through heavy water supplied by Los Alamos National Laboratory, with the gas flow set sufficiently low to avoid introducing large droplets of water into the plasma. A low dispersion plot of the spectrum is given in figure 1, illustrating the emission of OD between 1850 and 2750 cm^{-1} and the atmospheric emission of CO_2 with a head near 2390 cm^{-1}. The noise bursts at 2050, 3050 and 4050 cm^{-1} are attributed to harmonic frequencies of the plasma and are a considerable contribution to the noise in the spectrum. An intermediate dispersion plot of the spectrum is given in figure 2, containing the P and R branches of the 1–0 and 2–1 bands, and a high dispersion plot is given in figure 3 illustrating the rotational structure of the P branches of both bands.

The spectrometer and the details of the data transformation and reduction have been given in several earlier papers (Davis *et al* 1988 and Abrams *et al* 1989). The spectrometer was the one-meter Fourier transform spectrometer at the McMath Solar Telescope at the National Solar Observatory, Kitt Peak. The instrument was set to a resolving limit of 0·014 cm^{-1} and the observed spectrum was calibrated against the difference frequency laser measurement of the spectrum of the fundamental band performed by Amano (1984). Calibration with the argon lines present in the spectrum was not possible due to the presence of previously unmeasured pressure shifts. A line list was generated from the transformed interferogram using the interactive data-processing code DECOMP written by Brault, and adapted for use with IBM PC-compatible computers (Abrams 1989). Each identifiable OD line was fitted with a Voigt function to obtain accurate estimates of the wavenumber, intensity, width, damping parameter and equivalent width. The observed line positions and c − o (calculated minus observed) values are given in table 1 for the 1–0 band and table 2

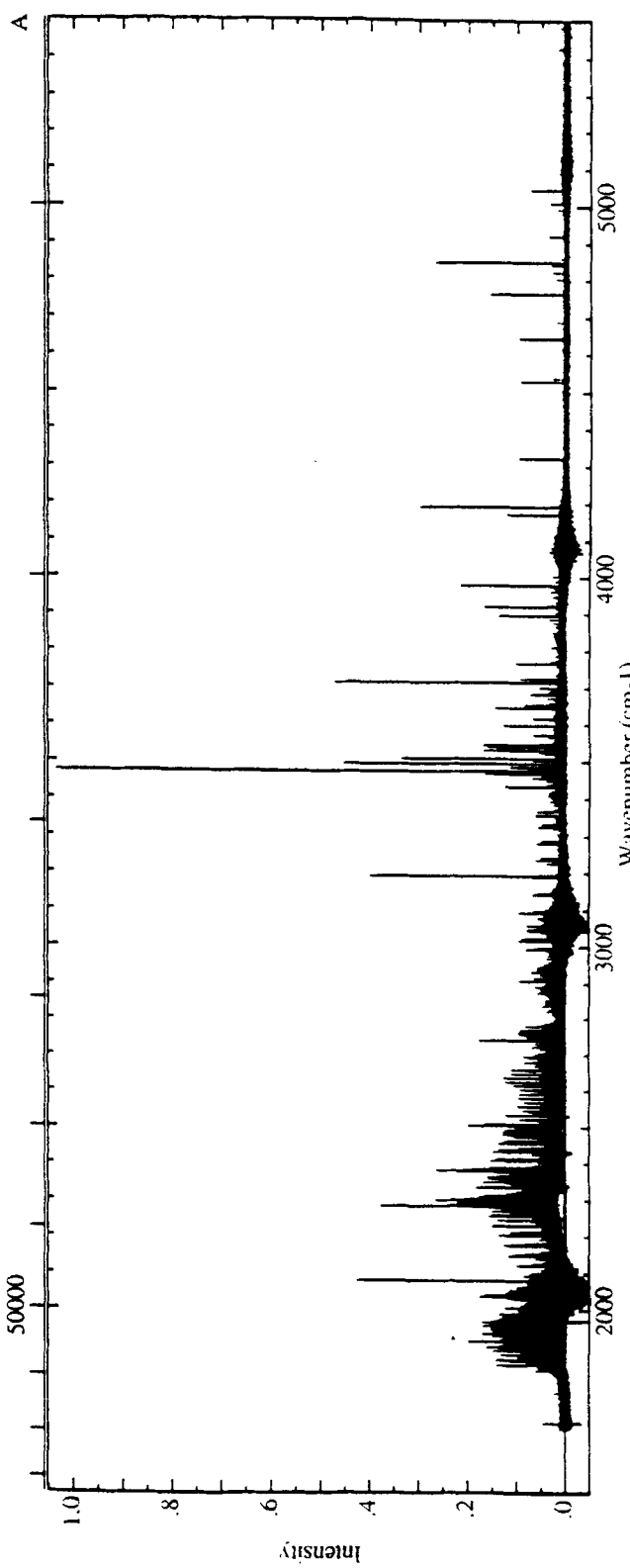

Figure 1. Low dispersion spectrum of an inductively coupled plasma illustrating the bands of OD and CO_2 in the near infrared and noise bursts at periodic intervals due to oscillations of the plasma.

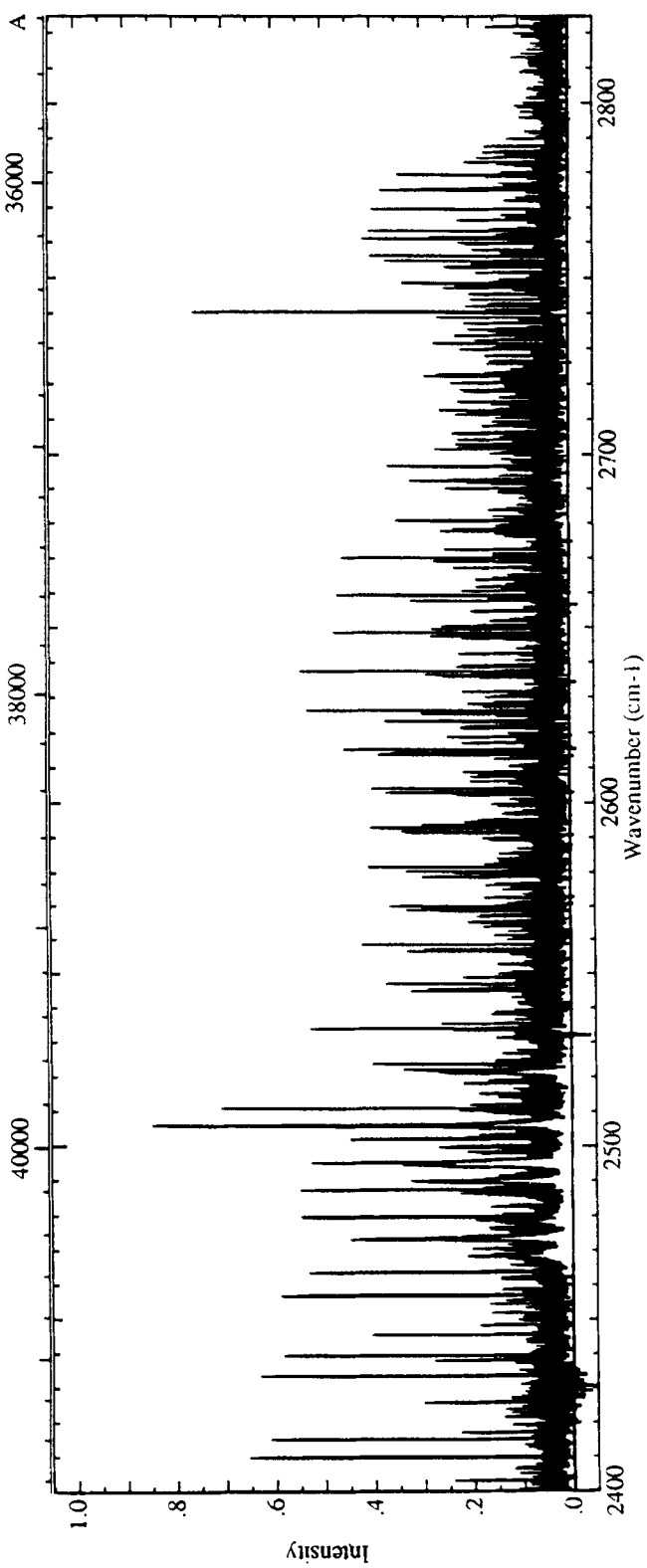

Figure 2. A portion of $\Delta v = 1$ sequence of OD illustrating the *P* and *R* branches of the 1–0 and 2–1 bands.

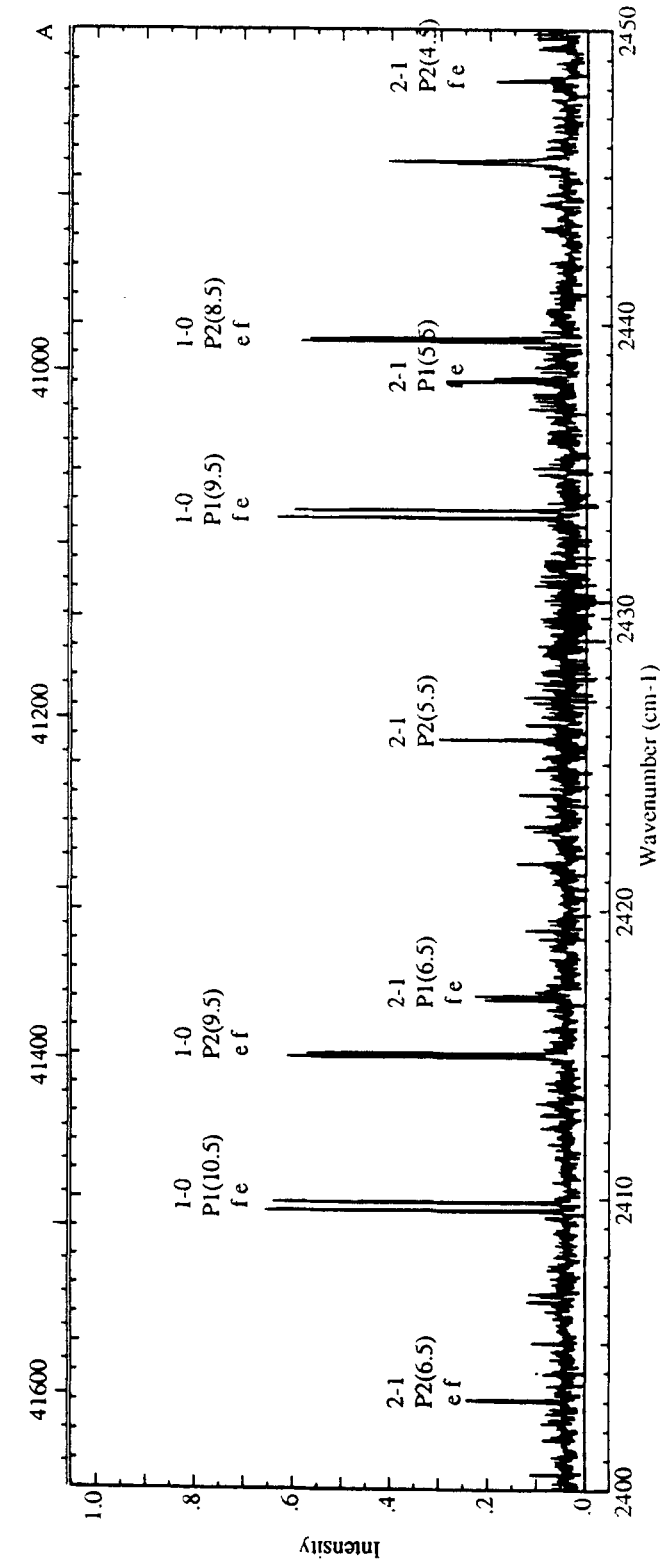

Figure 3. The *P* branches of the 1–0 and 2–1 bands of OD illustrating the resolved lambda doubling of each branch.

Table 1. Observed line positions of the 1–0 band of OD[a].

J	P_{1e}	c − o	P_{1f}	c − o	P_{2e}	c − o	P_{2f}	c − o
2·5					2578·6869	11	2578·6073	1
3·5	2565·2192	− 17	2565·1580	29	2556·4420	31	2556·3854	26
4·5	2544·7168	5	2544·6320	− 26	2533·7888	− 9	2533·7573	19
5·5	2523·6211	2	2523·5000	− 5	2510·7417	16	2510·7417	35
6·5	2501·9426	− 2	2501·7855	2	2487·3284	− 31	2487·3598	− 8
7·5	2479·7005	5	2479·5088	8	2463·5388	21	2463·6046	19
8·5	2456·9210	5	2456·6948	10	2439·3915	20	2439·4897	8
9·5	2433·6286	5	2433·3691	6	2414·8853	4	2415·0135	− 1
10·5	2409·8484	2	2409·5556	7	2390·0201	2	2390·1765	17
11·5	2385·6038	− 2	2385·2781	10	2364·8019	− 1	2364·9890	1
12·5	2360·9161	2	2360·5600	2	2339·2343	17	2339·4584	− 63
13·5	2335·8051	27	2335·4210	− 2	2313·3336	− 37	2313·5758	− 15
14·5	2310·2983	− 8	2309·8797	4	2287·0933	− 14	2287·3657	− 17
15·5	2284·3972	70	2283·9590	− 21	2260·5340	− 28	2260·8334	− 28
16·5	2258·1469	− 12	2257·6690	0	2233·6590	− 10	2233·9852	− 11
17·5	2231·5392	− 5	2231·0318	14	2206·4851	− 22	2206·8373	− 18
18·5	2204·6005	− 8	2204·0659	− 2	2179·0191	− 20	2179·3986	− 29
19·5	2177·3454	− 10	2176·7806	19	2151·2744	− 23	2151·6772	− 8
20·5	2149·7883	− 2	2149·1970	18	2123·2614	− 16	2123·6903	− 12
21·5	2121·9463	− 7	2121·3292	1	2094·9951	− 32	2095·4484	− 24
22·5	2093·8340	− 27	2093·1880	6				
23·5					2037·7398	− 24	2038·2302	92
24·5	2036·8404	30			2008·7680	67	2009·2983	17
25·5	2007·9998	− 28	2007·2619	o	1979·6052	− 12	1980·1502	19
26·5	1978·9352	− 21	1978·1871	31	1950·2313	59	1950·8100	− 24
27·5	1949·6852	o			1920·7075	o	1921·2701	78
28·5	1920·2153	o	1919·4132	7			1891·5736	7
29·5	1890·5729	o	1889·7571	− 68			1861·7140	− 60

J	R_{1e}	c − o	R_{1f}	c − o	R_{2e}	c − o	R_{2f}	c − o
1·5	2676·6739	− 53	2676·6739	o	2681·7066	1	2681·7788	− 51
2·5	2693·6365	o	2693·6365	o	2700·3012	− 21	2700·3415	− 6
3·5	2710·1460	− 36	2710·2191	− 42	2718·1350	− 84	2718·1350	60
4·5	2726·2243	− 7	2726·3209	− 12	2735·1795	54	2735·1795	− 74
5·5	2741·8381	− 56	2741·9514	− 5	2751·4793	2	2751·4412	− 5
6·5	2756·9329	41	2757·0738	19	2767·0200	− 3	2766·9538	30
7·5	2771·5049	4	2771·6629	− 9	2781·8138	12	2781·7356	− 52
8·5	2785·5049	32	2785·6805	0	2795·8740	− 8	2795·7626	65
9·5	2798·9166	24	2799·1016	33	2809·1947	49	2809·0738	43
10·5	2811·7094	54	2811·9098	24	2821·7951	18	2821·6656	− 56
11·5			2824·0812	8				
12·5			2835·6005	− 38				

[a] c − o is scaled by 10^4, and the letter o indicates that a measured line was omitted from the final calculation.

Table 2. Observed line positions of the 2–1 band of OD[a].

J	P_{1e}	c − o	P_{1f}	c − o	P_{2e}	c − o	P_{2f}	c − o
2·5	2498·0442	o	2498·0443	o	2491·9448	o	2491·8665	o
3·5	2478·6690	−24	2478·6203	24	2470·3087	−5	2470·2484	30
4·5	2458·6988	22	2458·6155	21	2448·2567	46	2448·2346	−31
5·5	2438·1482	12	2438·0373	−38	2425·8222	0	2425·8222	−4
6·5	2417·0274	4	2416·8796	−14	2403·0139	o	2403·0381	−16
7·5	2395·3535	10	2395·1642	70	2379·7850	o	2379·8893	−61
8·5	2373·1525	−4	2372·9333	20	2356·2744	−4	2356·3592	65
9·5	2350·4561	o	2350·1947	−4				
10·5	2327·2479	60	2326·9728	−10	2308·1013	0	2308·2411	o
11·5	2303·6070	−26	2303·2924	−18	2283·4765	87	2283·6639	12
12·5	2279·5172	−5	2279·1712	7	2258·5247	−14	2258·7290	25
13·5	2255·0119	−7	2254·6366	−8	2233·2220	9	2233·4566	22
14·5	2230·1076	−6	2229·7012	4	2207·5909	12	2207·8564	−12
15·5	2204·8241	−19	2204·3889	−17	2181·6407	−5	2181·9288	12
16·5	2179·1743	−3	2178·7095	4	2155·3757	10	2155·6900	29
17·5	2153·1808	−18	2152·6877	−14	2128·8089	34	2129·1570	−27
18·5	2126·8525	6	2126·3306	14			2102·3250	2
19·5	2100·2089	26	2099·6628	−2	2074·8180	o	2075·2214	−48
20·5	2073·2758	−66	2072·6998	−70				
21·5								
22·5			2017·9155	−59	1991·8661	−37	1992·3222	55
23·5	1990·7759	40	1990·1161	76	1963·7267	−1	1964·2158	−6
24·5	1962·7735	11	1962·0888	40	1935·3702	−14	1935·8806	−4
25·5	1934·5331	37	1933·8294	4	1906·8024	o	1907·3377	−37
26·5	1906·0786	3	1905·3449	o				
27·5	1877·4134	−5	1876·6596	o				
28·5	1848·5519	−12	1847·7075	o				

J	R_{1e}	c − o	R_{1f}	c − o	R_{2e}	c − o	R_{2f}	c − o
0·5					2573·1654	31	2573·2566	−30
1·5	2587·1633	39	2587·2008	−84	2591·9140	53	2591·9856	−7
2·5	2603·6279	−21	2603·6657	59	2609·9483	−54	2609·9913	−68
3·5	2619·6535	22	2619·7205	34	2627·2316	o	2627·2316	32
4·5	2635·2439	−49	2635·3300	−3	2643·7417	8	2643·7417	−96
5·5	2650·3444	49	2650·4498	o	2659·5227	−63	2659·4780	30
6·5	2664·9608	−43	2665·0902	−25	2674·5507	−27	2674·4838	59
7·5	2679·0352	−45	2679·1958	o	2688·8290	o	2688·7632	30
8·5	2692·5442	−3	2692·7039	31	2702·4298	o	2702·3170	2
9·5	2705·4751	−44			2715·2858	o		
10·5					2727·3826	o		

[a] c − o is scaled by 10^4, and the letter o indicates that a measured line was omitted from the final calculation.

for the 2–1 band. We have labelled the lines with the traditional F_1 or F_2, e or f notation.

3. Theory

Effective Hamiltonians for the interpretation of the spectra of diatomic molecules begin with approximating the exact Hamiltonian by

$$H = H_0 + H_{ROT} + H_{CD} + H_{FS} + H_{LD} + H_{CDLD} \tag{1}$$

where H_0 includes all the rotation independent terms of the Born-Oppenheimer approximation and involves only electronic and vibrational quantum numbers. The hyperfine splitting is unresolved in the infrared and consequently the hyperfine interaction terms have been omitted. H_{ROT} is the rotational energy and H_{CD} includes the centrifugal distortions of the rotational energy. The term H_{FS} describes the fine structure interactions and H_{LD} and H_{CDLD} describe the lambda doubling interaction and its centrifugal distortion respectively. Zare *et al* (1973) have evaluated an effective Hamiltonian using the unique perturber approximation (UPA) and Brown *et al* (1978, 1979) have developed a tensor method that introduces the interactions with other states directly. We have used the tensor Hamiltonian method, however we include the results from a calculation based on the UPA for comparison with earlier results.

The rotational Hamiltonian H_{ROT} is

$$H_{ROT} = BT^1(\mathbf{R})\, T^1(\mathbf{R}) = B\mathbf{R}^2 \tag{2}$$

where B is the rotational parameter. The centrifugal distortion corrections to the rotational energy are

$$H_{CD} = -D\mathbf{R}^4 + H\mathbf{R}^6 - L\mathbf{R}^8 \tag{3}$$

where D, H, and L are the quartic, sextic, and octic distortion parameters. The third term H_{FS} includes the interactions between the orbital, spin and rotational angular momenta of the electrons

$$H_{FS} = H_{SS} + H_{SO} + H_{SR}. \tag{4}$$

In all $^2\Pi$ states the spin–spin interaction energy is rigorously zero. The spin-orbit Hamiltonian H_{SO} can be expressed in tensor form as

$$H_{SO} = AT^1_0(\mathbf{L})\, T^1_0(\mathbf{S}) + \frac{A_D}{2}[\mathbf{R}^2\, T^1_0(\mathbf{L})\, T^1_0(\mathbf{S}) + T^1_0(\mathbf{L})\, T^1_0(\mathbf{S})\mathbf{R}^2] + A_H[\mathbf{R}^4 T^1_0(\mathbf{L})\, T^1_0(\mathbf{S}) + T^1_0(\mathbf{L})\, T^1_0(\mathbf{S})\mathbf{R}^4] \tag{5}$$

where A is the spin-orbit interaction parameter, and A_D and A_H are the centrifugal corrections to A. The spin-rotation Hamiltonian H_{SR} is given by

$$H_{SR} = \gamma T^1(\mathbf{N})\, T^1(\mathbf{S}) = \gamma T^1(\mathbf{J} - \mathbf{S})\, T^1(\mathbf{S}) \tag{6}$$

and the lambda doubling Hamiltonian has the form

$$H_{LD} = \sum_{q=\pm 1} \exp[-2iq\phi]\{[-qT^2_{2q}(\mathbf{J},\mathbf{J}) + (p+2q)T^2_{2q}(\mathbf{J},\mathbf{S})]\} \tag{7}$$

where p and q are the lambda doubling parameters as defined by Mulliken and Christy (1931) and ϕ is the azimuthal coordinate. The centrifugal distortions of the lambda doubling interaction are

$$(H_{LD})^4_{CD} = \sum_{q=\pm 1} \exp[-2iq\phi]\left\{-\frac{q_D}{2}[T^2_{2q}(\mathbf{J},\mathbf{J})\mathbf{R}^2 + \mathbf{R}^2 T^2_{2q}(\mathbf{J},\mathbf{J})] + \frac{1}{2}(p_D + 2q_D)[T^2_{2q}(\mathbf{J},\mathbf{S})\mathbf{R}^2 + \mathbf{R}^2 T^2_{2q}(\mathbf{J},\mathbf{S})]\right\} \quad (8)$$

and

$$(H_{LD})^6_{CD} = \sum_{q=\pm 1} \exp[-2iq\phi]\left\{-\frac{q_H}{2}[T^2_{2q}(\mathbf{J},\mathbf{J})(\mathbf{R}^2)^2 + (\mathbf{R}^2)^2 T^2_{2q}(\mathbf{J},\mathbf{J})] + \frac{1}{2}(p_H + 2q_H)[T^2_{2q}(\mathbf{J},\mathbf{S})(\mathbf{R}^2)^2 + (\mathbf{R}^2)^2 T^2_{2q}(\mathbf{J},\mathbf{S})]\right\} \quad (9)$$

where q_D and q_H are the centrifugal corrections to q, and p_D and p_H are the corresponding corrections to p. In each of the fine structure and Λ-doubling terms, the spherical tensor notation is consistent with the notation used by Edmonds (1974). The components q refer to the molecule-fixed components of the various angular momenta. The lambda doubling terms possess a phase factor $\exp(-2iq\phi)$, and the allowed values of $q = \pm 1$ determine a selection rule of $\Delta\Lambda = \mp 2$ between case (a) basis functions. For $^2\Pi$ states transitions between the lambda doubled energy levels connect states with $\Lambda = 1$ and $\Lambda = -1$.

Table 3. Matrix elements of the tensor Hamiltonian for a $^2\Pi$ state in an *e/f* symmetrized, Hund's case (a) Basis set[a].

T	1,1	1	p_D	2,2	$\mp 0.5(J+0.5)(z+2)$
	2,2	1		1,2	$\pm 0.25z^{0.5}(J+0.5)$
A	1,1	0.5	p_H	2,2	$\mp 0.5(z+4)(J+0.5)^3$
	2,2	-0.5		1,2	$\pm 0.5z^{0.5}(J+0.5)^3$
A_D	1,1	$0.5z$	q	2,2	$\mp(J+0.5)$
	2,2	$-0.5(z+2)$		1,2	$\pm 0.5z^{0.5}(J+0.5)$
A_H	1,1	z^2	q_D	1,1	$\mp 0.5z(J+0.5)$
	2,2	$-(z+2)^2$		2,2	$\mp 0.5(3z+4)(J+0.5)$
	1,2	$z^{0.5}$		1,2	$\pm 0.5z^{0.5}(z+4)(J+0.5)$
B	1,1	z	q_H	1,1	$\mp z(J+0.5)^3$
	2,2	$z+2$		2,2	$\mp 2(z+2)(J+0.5)^3$
	1,2	$-z^{0.5}$		1,2	$\pm 0.5z^{0.5}(z+4)(J+0.5)^3$
D	1,1	$-z(z+1)$	γ	2,2	-1
	2,2	$-(z+1)(z+4)$		1,2	$0.5z^{0.5}$
	1,2	$2z^{0.5}(z+1)$	γ_D	1,1	$-0.5z$
H	1,1	$z(z+1)(z+2)$		2,2	$-0.5(3z+4)$
	2,2	$(z+1)(z^2+8z+8)$		1,2	$0.5z^{0.5}(z+2)$
	1,2	$-z^{0.5}(z+1)(3z+4)$	γ_H	1,1	$-z(z+1)$
L	1,1	$-z(z+1)^2(z+4)$		2,2	$2(z+1)(z+2)$
	2,2	$-(z+1)^2(z^2+12z+16)$		1,2	$0.5z^{0.5}(z^2+5z+4)$
	1,2	$4z^{0.5}(z+1)^2(z+2)$			
p	2,2	$\mp 0.5(J+0.5)$			

[a]Notation: $z = (J+\frac{1}{2})^2 - 1 = (J-\frac{1}{2})(J+\frac{3}{2})$ state notation: $1 = {}^2\Pi_{3/2}$, $2 = {}^2\Pi_{1/2}$. When specified, the upper sign refers to *e* sublevels and the lower sign refers to *f* sublevels.

Table 4. Matrix elements of the UPA Hamiltonian for a $^2\Pi$ state in an *e/f* symmetrized, Hund's case (a) Basis set[a].

T	1,1	1	p_D	1,2	$-0.25z^{0.5}J(J+1)$
	2,2	1		2,2	$0.5(1\mp(J+0.5))J(J+1)$
A	1,1	0.5	p_H	1,2	$-0.25z^{0.5}J^2(J+1)^2$
	2,2	-0.5		2,2	$0.5(1\mp(J+0.5))J^2(J+1)^2$
A_D	1,1	$0.5(z-1)$	q	1,1	$0.5z$
	2,2	$-0.5(z+1)$		2,2	$0.5(z+2\mp(J+0.5))$
A_H	1,1	$0.25(3(z-1)^2+z)$		1,2	$\pm 0.5z^{0.5}(-1\pm(J+0.5))$
	2,2	$-0.25(3(z+1)^2+z)$	q_D	1,1	$0.5zJ(J+1)$
	1,2	$0.5z^{0.5}$		2,2	$0.5(z+2\mp(J+0.5))J(J+1)$
B	1,1	$z-1$		1,2	$\pm 0.5z^{0.5}(-1\pm(J+0.5))J^2(J+1)^2$
	2,2	$z+1$	q_H	1,1	$0.5zJ^2(J+1)^2$
	1,2	$-z^{0.5}$		2,2	$0.5(z+2\mp(J+0.5))J^2(J+1)^2$
D	1,1	$-(z-1)^2-z$		1,2	$\pm 0.5z^{0.5}(-1\pm(J+0.5))J^2(J+1)^2$
	2,2	$-(z+1)^2+z$	γ	1,1	0.5
	1,2	$2z^{1.5}$		2,2	-0.5
H	1,1	$(z-1)^3+z(3z-1)$		1,2	$0.5z^{0.5}$
	2,2	$(z+1)^3+z(3z+1)$	γ_D	1,1	$0.5J(J+1)$
	1,2	$-(3z^2+z+1)z^{0.5}$		2,2	$-0.5J(J+1)$
L	1,1	$(z-1)^4+z(6z^2-3z+2)$		1,2	$\pm 0.5z^{0.5}J^2(J+1)^2$
	2,2	$(z+1)^4+z(6z^2+5z+2)$	γ_H	1,1	$-0.5J^2(J+1)^2$
	1,2	$-4z^{1.5}(z^2+z+1)$		2,2	$-0.5J^2(J+1)^2$
o	2,2	1		1,2	$0.5z^{0.5}J^2(J+1)^2$
p	1,2	$-0.25z^{0.5}$			
	2,2	$0.5(1\mp(J+0.5))$			

[a]Notation: $z=(J+\frac{1}{2})^2-1=(J-\frac{1}{2})(J+\frac{3}{2})$ state notation: $1=^2\Pi_{3/2}$, $2=^2\Pi_{1/2}$. When specified, the upper sign refers to *e* sublevels and the lower sign refers to *f* sublevels.

The matrix elements of the tensor Hamiltonian are given in table 3. The UPA Hamiltonian parameters (table 4) differed from those used by Amiot *et al* (1981) in the presence of a minus sign in the *L*-type parameters.

4. Analysis and data reduction

The data are fitted directly using deperturbation methods to derive physically meaningful molecular parameters which may be used to predict the wavenumbers of new transitions. The procedure and the computer code follow the methods outlined by Field (1971), Albritton *et al* (1976), and Lefebvre-Brion and Field (1986). The states are modeled by a Hamiltonian written in terms of equilibrium molecular parameters. Diagonalization of the secular determinant of the model Hamiltonian generates the term values of the upper and lower states, from which spectral wavenumbers can be computed directly. Initially the Hamiltonian is evaluated using trial parameters obtained from previous analyses and then the predicted line positions are compared to the observed line positions. A nonlinear least square fitting procedure allows the molecular parameters to be adjusted until an optimal fit is achieved.

Initially each branch is individually fit to a polynomial in J using the interactive computer code ANALYSIS developed by Pecyner and Davis (1988) for the analysis of medium to heavy diatomic spectra. Such a fitting method is essential for correctly assigning the F_2 lambda doubling components which cross through each other in the spectra. Lines which deviate from the expected positions by more than three standard deviations (3σ) are purged from the fit before the fit is recalculated. The branches are then fit together using NLFIT to obtain initial parameters for each band and to find perturbed lines.

A global fit, using a nonlinear least square procedure, is used to derive equilibrium parameters. In the global fitting process all the lines are used in the successive iterations (no lines were purged as the fit progressed). Trial parameters were developed and used to set up the Hamiltonians of the upper and lower states for the vibrational levels with v between 0 and 2. Diagonalization generates F_1 and F_2 sublevels for each J-value of the upper and lower states, from which calculated line positions are obtained for the transitions. Direct comparison of the calculated wavenumbers with the corresponding experimentally observed line positions generates corrections to the molecular parameters. The corrections permit a new set of term values to be calculated and the procedure is repeated until convergence is achieved. In the present case, two iterations are sufficient to obtain convergence, the ratio of the standard deviations produced by the first and second iterations is a good measure of the rate of convergence and is on the order of 10 or more. When the data of Amiot *et al* (1981) are combined with our data for a global fit, systematic vibrational dependance of centrifugal distortion parameters has been lost. So, we are constrained to use only the data reported in the present work.

The final global fit yielded a standard deviation of 0·0032 cm^{-1} for 245 of the 257 observed lines when the tensor Hamiltonian is used; similarly, when the UPA Hamiltonian is used the standard deviation was 0·0032 cm^{-1}. The resultant molecular parameters are given in table 5.

Table 5a. Tensor Hamiltonian parameters for the $X\,^2\Pi_i$ state of OD[a].

Parameter	$v=0$	$v=1$	$v=2$
T_v		2632·33512(99)	5176·37545(12)
A	−139·04714(73)	−139·23931(72)	−139·42905(72)
B	9·878621(18)	9·603064(19)	9·330473(20)
$D \times 10^4$	5·373(11)	5·290(11)	5·213(12)
$H \times 10^8$	[2·0233]	[1·9168]	[1·8267]
$A_D \times 10^3$	−7·620(51)	−7·184(51)	−6·759(52)
p	0·12611(15)	0·12214(15)	0·11820(14)
$p_D \times 10^5$	−1·98(88)	−2·05(94)	−2·17(99)
$q \times 10^2$	−1·0922(28)	−1·0544(29)	−1·0169(31)
$q_D \times 10^6$	2·3(15)	2·3(16)	2·3(17)
$q_H \times 10^{10}$	[−1·46]	[−1·18]	[−1·46]
$L \times 10^{13}$	[7·74]	[5·44]	[4·97]
$A_H \times 10^7$	[8·85]	[8·68]	[7·84]

[a] All values are given in reciprocal centimeters, and the error quoted is one standard deviation in the last decimal place. The standard deviation is 0·0032 cm^{-1} for reproducing individual spectral lines. Bracketed quantities are held constant during the fitting process.

Table 5b. UPA Hamiltonian parameters for the $X\,^2\Pi_i$ state of OD[a].

Parameter	$v=0$	$v=1$	$v=2$
T_e		2632·05936(74)	5175·82788(10)
A	−139·21509(55)	−139·40846(55)	−139·59938(55)
B	9·883039(16)	9·607346(16)	9·334593(17)
$D \times 10^4$	5·3868(81)	5·3057(85)	5·2304(91)
$H \times 10^8$	[2·006]	[1·934]	[1·861]
$A_D \times 10^4$	−6·43(28)	−6·21(31)	−6·00(28)
p	0·12555(10)	0·12170(10)	0·1176(11)
$p_D \times 10^5$	−1·39(58)	−1·46(61)	−1·55(64)
$q \times 10^2$	−1·0808(18)	−1·0444(19)	−1·0068(20)
$q_D \times 10^6$	1·91(93)	1·85(99)	1·7(11)
$q_H \times 10^{10}$	[−1·52]	[−1·46]	[−1·46]
$L \times 10^{13}$	[7·06]	[6·40]	[6·40]
$A_H \times 10^7$	[2·14]	[1·21]	[1·21]

[a] All values are given in reciprocal centimeters, and the error quoted is one standard deviation in the last decimal place. The standard deviation is 0·0032 cm^{-1} for reproducing individual spectral lines. Bracketed quantities are held constant during the fitting process.

The results obtained with the tensor and UPA Hamiltonians are compared in table 6b. Theoretical relations between the tensor parameters and those derived under the unique perturber approximation have been given by Brown *et al* (1979) and are summarized in table 6a. The tilded parameters are tensor parameters and the superscript π denotes unique perturber parameters. The relationship between the electronic-vibrational energy parameter is included to define explicitly the difference between the energy levels calculated with the two methods: the factor of B_v^π compensates for the difference between the matrix elements of the rotational Hamiltonian given in tables 3 and 4. The parameter o_v^π is calculated from the relation

$$o_v^\pi = p_v^\pi A_v^\pi / 8B_v^\pi \tag{10}$$

obtained by Veseth (1971) using the unique perturber approximation.

The relations permit the calculation of tensor parameters from the measured UPA parameters; differences between the derived and calculated parameters are given in table 6b. The systematic differences between the observed B values and the derived B values have been attributed (Amiot *et al* 1981) to the incorrect equivalence of matrix elements of $\mathbf{R}^2$ (UPA) and $\mathbf{N}^2$ (tensor) that leads to the expression for $\tilde{B}_{nv}$ in table 6a. The differences are nearly equal to $2D_v^\pi$. As predicted the other rotational constants D, H, and L obtained with the two Hamiltonians are in reasonable agreement. The spin-orbit parameters A, and A_D vary smoothly in both calculations and the differences between the calculated and derived parameters is within the accuracy of the measurement. The lambda-doubling parameters, p and q, are nearly identical and the centrifugal distortion parameters p_D and q_D are of the same order of magnitude. The relative consistency of the two sets of Hamiltonian parameters is reflected in table 6b by the magnitude of the differences, all of which are smaller than those tabulated by Amiot *et al*.

Table 6a. Relation between tensor and UPA Hamiltonian parameters for a $^2\Pi$ electronic state[a].

$$\tilde{T}_{ne} + \tilde{G}_{nv} = T_v^\pi - B_v^\pi + \frac{1}{2}o_v^\pi + (A_v^\pi - o_v^\pi)\left\{\frac{p_v^\pi}{4\{A_v^\pi - o_v^\pi - 2B_v^\pi - q_v^\pi\}}\right\}$$

$$\tilde{A}_{nv} = (A_v^\pi - o_v^\pi)\left\{\frac{p_v^\pi}{2\{A_v^\pi - o_v^\pi - 2B_v^\pi - q_v^\pi\}}\right\}$$

$$\tilde{A}_{Dnv} = A_{Dv}^\pi + \left(B_v^\pi + \frac{1}{2}q_v^\pi\right)\left\{\frac{p_v^\pi}{\{A_v^\pi - o_v^\pi - 2B_v^\pi - q_v^\pi\}}\right\}$$

$$\tilde{B}_{nv} = B_v^\pi + \frac{1}{2}q_v^\pi$$

[a] Assuming $\tilde{\gamma}_{nv} = 0$. $\tilde{D}_{nv} = D_v^\pi$, $\tilde{p}_{nv} = p_v^\pi$, $\tilde{q}_{nv} = q_v^\pi$,

Table 6b. Differences between observed and calculated tensor parameters (cm^{-1}).

Vibrational level	0	1	2
$A_{nv} - (\tilde{A}_{nv})_{CALC} \times 10^3$	−1·50	−1·8	−2·0
$B_{nv} - (\tilde{B}_{nv})_{CALC} \times 10^4$	9·8	9·4	9·1
$A_{Dnv} - (\tilde{A}_{Dnv})_{CALC} \times 10^4$	−4·6	−8·1	−7·7
$p_D - p_v^\pi \times 10^4$	1·4	1·6	1·7
$q_D - q_v^\pi \times 10^4$	−5·2	−4·3	−4·4
$D - D_v^\pi \times 10^4$	−1·1	−1·0	−1·0

5. Conclusions

We have observed new spectral lines in the vibration-rotation spectrum of the OD radical, including additional lines of the 1–0 band and the 2–1 band has been observed for the first time. These spectral lines were subjected to a nonlinear fit using a tensor Hamiltonian to determine improved molecular parameters with a standard deviation of 0·0032 cm^{-1}. The parameters determined with the nonlinear fit display a slow variation with vibrational quantum number, in particular the values of A_D for $v = 0$, 1 and 2 are all negative whereas in earlier works these was no pattern in the variation of the equilibrium centrifugal distortion parameters. The utility of low v and high J spectral production by the inductively coupled plasma discharge facilitated the evaluation of improved centrifugal distortion molecular parameters.

Acknowledgements

One of the authors (SPD) gratefully acknowledges the financial support of a National Science Foundation grant and a grant from the Institute of Geophysics and Planetary Physics. The generous technical support of the Kitt Peak National Solar Observatory

staff is also acknowledged, particularly James W Brault. In addition we acknowledge the assistance of Lynda M Faires in the operation of the inductively coupled plasma discharge.

M C Abrams was partially supported by grants from the Institute for Geophysics and Planetary Physics, Los Alamos National Laboratory and the NASA Ames Research Center.

References

Abrams M C, Davis S P and Engleman Jr R 1989 *Optics News* **15** A55

Abrams M C 1989 *High resolution Fourier transform spectroscopy*, Technical Digest Series, (Washington DC: Optical Society of America) Vol. 6, 58–59

Albritton D L, Schmeltekopf A L and Zare R N 1976 in *Molecular Spectroscopy. Modern Research* (ed.) K Narahari Rao (New York: Academic Press) Vol. II pp. 1–67

Amano T 1984 *J. Mol. Spectrosc.* **103** 436

Amiot C, Maillard J P and Chauville J 1981 *J. Mol. Spectrosc.* **87** 196

Brown J M, Kaise M, Kerr C M L and Milton D J 1978 *Mol. Phys.* **36** 553

Brown J M, Kerr C M L, Wayne F D, Evenson K M and Radford H E 1981 *J. Mol. Spectrosc.* **86** 544

Brown J M and Schubert J E 1982 *J. Mol. Spectrosc.* **95** 194

Brown J M, Colbourn E A, Watson J K G and Wayne F D 1979 *J. Mol. Spectrosc.* **74** 294

Davis S P, Abrams M C, Sandalphon Brault J W and Rao M L P 1988 *J. Opt. Soc. Am.* **B5** 1838

Edmonds A R 1974 *Angular momentum in quantum mechanics* (London and New York: Oxford University Press Clarendon)

Field R W 1971 Spectroscopy and perturbation analysis in excited states of CO and CS Ph.D. thesis (Harvard University, Cambridge, Mass)

Lefebvre-Brion H and Field R W 1986 *Perturbations in the spectra of diatomic molecules* (New York: Academic Press)

Mulliken R S and Christy A 1931 *Phys. Rev.* **38** 87

Pecyner R and Davis S P 1988 *Appl. Opt.* **27** 3775

Veseth L 1971 *J. Mol. Spectrosc.* **38** 228

Zare R N, Schmeltekopf A L, Harrop W J and Albritton D L 1973 *J. Mol. Spectrosc.* **46** 37